

Published in the ApJ Letters, vol. 733, L1, 2011 May 20

A New Look at the Old Star Cluster NGC 6791

I. Platais

*Department of Physics and Astronomy, The Johns Hopkins University, Baltimore, MD
21218, USA;*

imants@pha.jhu.edu

K. M. Cudworth

Yerkes Observatory, The University of Chicago, Williams Bay, WI 53191, USA

V. Kozhurina-Platais

Space Telescope Science Institute, 3700 San Martin Drive, Baltimore, MD 21218, USA

D. E. McLaughlin

*Astrophysics Group, Lennard-Jones Laboratories, Keele University, Keele, Staffordshire
ST5 5BG, UK*

S. Meibom

*Harvard-Smithsonian Center for Astrophysics, 60 Garden Street, Cambridge, MA 02138,
USA*

and

C. Veillet

Canada-France-Hawaii Telescope Corporation, Kamuela, HI 96743, USA

ABSTRACT

We present comprehensive cluster membership and $g'r'$ photometry of the prototypical old, metal-rich Galactic star cluster NGC 6791. The proper-motion catalog contains 58,901 objects down to $g' \sim 24$, limited to a circular area of radius $30'$. The highest precision of the proper motions is 0.08 mas yr^{-1} . Our proper motions confirm cluster membership of all main and also some rare constituents

of NGC 6791. The total number of probable cluster members down to $g' = 22$ ($M_V \sim +8$) is ~ 4800 , corresponding to $M_{\text{tot}} \approx 5000 M_\odot$. New findings include an extended horizontal branch in this cluster. The angular radius of NGC 6791 is at least $15'$ (the effective radius is $R_h \simeq 4.4'$ while the tidal radius is $r_t \simeq 23'$). The luminosity function of the cluster peaks at $M_{g'} \sim +4.5$ and then steadily declines toward fainter magnitudes. Our data provide evidence that differential reddening may not be ignored in NGC 6791.

Subject headings: astrometry — open clusters and associations: general — open clusters and associations: individual (NGC 6791) — proper motions

1. Introduction

NGC 6791 is an extreme Galactic star cluster with an old age of ~ 8 Gyr (Grundahl et al. 2008), a high metallicity $[\text{Fe}/\text{H}] = +0.30$ (Boesgaard et al. 2009), and an unusual orbit that periodically brings it close to the bulge of the Milky Way (Bedin et al. 2006). Kinman (1965) was the first to provide an estimate for the total mass of NGC 6791: $\sim 3700 M_\odot$ down to $V = 20$, confirmed by Kaluzny & Udalski (1992). It is widely acknowledged that NGC 6791 is one of the most massive old open clusters in our Galaxy.

As indicated by the discovery of several extremely blue subdwarfs (Kaluzny & Udalski 1992) and the presence of a prominent red clump, morphology of the color-magnitude diagram (CMD) for NGC 6791 is complex. The proposed enhanced mass loss along the red giant branch (RGB) appears to explain the presence of hot subdwarfs and the abnormally young 2.4 Gyr white dwarf cooling age (Kalirai et al. 2007). Recently, Twarog et al. (2011) reported that the CMD in the inner part of NGC 6791 ($R < 2'$) is somewhat different from that in its outer part ($2' < R < 5'$). Specifically, there is a dichotomy near the main-sequence turnoff, which the authors interpret as a result of protracted star formation.

This cluster is critically important to understanding a number of issues, such as stellar evolution and population synthesis at high metallicity in the Milky Way and other galaxies, specifically, in ellipticals and in spirals with bulges. Due to its relative proximity and its abundance of members, NGC 6791 provides perhaps the best opportunity for detailed studies of old and metal-rich populations. Despite a rich array of extant photometric and spectroscopic studies, however, the basic knowledge of cluster membership by kinematic means has been limited until now to radial velocities of a few dozen bright stars (e.g., Scott et al. 1995; Carraro et al. 2006) and preliminary proper motions for a few thousand stars (Cudworth & Anthony-Twarog 1993; Bedin et al. 2006). NGC 6791 is located in the

field of view (FOV) of NASA’s *Kepler* mission (Borucki et al. 2010) and is one of the targets of the Kepler Open Cluster Study (Meibom & Kepler Team 2010). It is also one of the clusters in the WIYN Open Cluster Study¹ (Mathieu 2000) – again, largely owing to its extreme properties.

This Letter presents the highlights of a new and comprehensive proper-motion study of NGC 6791, based upon the selection of exquisite deep photographic plates in combination with a decade of CCD imaging. The resulting proper motions provide nearly definite cluster membership for stars brighter than $g' \sim 22$ and, thus, unveil most of the cluster’s population with unprecedented clarity.

2. Astrometry and Photometry

NGC 6791 is a rich but faint star cluster with a main-sequence turnoff at $V \sim 17.5$ (Stetson et al. 2003, hereafter SBG), thus requiring relatively long exposures even with 3–4 m class telescopes. Fortunately, there are deep photographic plates dating back to 1961. We selected the best 33 plates (assessed by the depth and sharpness of images) taken with the Lick 3 m and the Kitt Peak National Observatory (KPNO) 4 m telescopes. These plates were digitised using the Space Telescope Science Institute’s GAMMA II multi-channel scanning microdensitometer. The second epoch includes 66 frames obtained with the NOAO CCD Mosaic Imager at the KPNO 4 m telescope in 1999–2007. The finest 24 CCD mosaic frames in $g'r'$ filters (1, 30, and 300 s exposures) were obtained in 2009 November with MegaCam at the 3.6 m Canada-France-Hawaii Telescope. These frames served for construction of a master catalog consisting of 128,771 objects down to $g' \sim 25$ and over an FOV of 1 deg². We put positions on the system of the UCAC3 catalog (Zacharias et al. 2010) and calculated proper motions on this system using the iterative central-plate-overlap algorithm (e.g., Jones & Walker 1988). The final catalog contains a total of 58,901 objects down to $g' \sim 23.8$ over a smaller area of ~ 0.8 deg², defined by a circular FOV (with radius 30') of the KPNO photographic plates. The highest precision of our proper motions is 0.08 mas yr⁻¹. Cluster membership probabilities are calculated using the frequency functions for cluster and field stars, obtained in selected magnitude and spatial ranges. Discrimination between cluster members and field stars is excellent down to $g' \sim 22$. Details of the astrometric reductions and the description of the catalog itself will appear elsewhere (Platais et al., in preparation).

For photometry, we used only the MegaCam images in $g'r'$ filters. The central part of NGC 6791 is fairly crowded, often resulting in blended images. We note that all Mega-

¹This is WOCS paper 46 of the WIYN Open Cluster Study.

Cam images are preprocessed with Elixir which, besides the standard steps, also normalizes the instrumental photometric zeropoint between the chips (see Magnier & Cuillandre 2004; Clem et al. 2008). The short, 1 s exposures obtained in subarcsecond seeing were instrumental in constructing an initial catalog of positions and aperture photometry (MAG_AUTO magnitudes from SExtractor). Magnitudes from longer exposures were added only if they matched specified tolerances on position and magnitude. In this way it was possible to minimize the deleterious effects of image blending. Nevertheless, image blending and CCD chip edge effects may occasionally yield stellar colors that are significantly off. Our instrumental photometry was put into the standard $g'r'$ system by employing the extant secondary photometric sequence in NGC 6791 (Clem et al. 2008). The rms error of the calibrating fits is 0.02 mag. On average, a calibrated g' magnitude near the main-sequence turnoff of NGC 6791 is ~ 0.41 mag fainter than that in V .

3. New Census of NGC 6791

One of the most comprehensive photometric surveys of NGC 6791 is that by SBG, who also provide extensive lists of bright stars, red giants, and faint blue stars in this cluster—all possible or likely members. Now, we are in a position to provide nearly definite star-by-star kinematic membership, with a caveat that stars with blended images may not appear in our proper motion catalog or, if they do, may be biased. An example of such a case is the eclipsing binary V20 – a definite cluster member (Grundahl et al. 2008) but incorrectly classed as a field star in our catalog. Its measured proper motion is apparently corrupted by the adjacent star ($\Delta_{\text{pos}}=2''$) in the amount of $\sim 6\sigma_{\mu}$. The CMD in Figure 1 shows the cleanest and the most complete census of NGC 6791 to date. It contains all stars with cluster membership probability $P_{\mu} \geq 19\%$, as well as stars with $19\% > P_{\mu} > 1\%$ but located on the main sequence, all within a radius $R \leq 15'$ from the cluster center – very close to that adopted by Twarog et al. (2011). The cluster membership probabilities for peripheral members of NGC 6791 ($R > 15'$) are less reliable because of the overwhelming number of field stars and numerical instabilities in finding the cluster population. Hence, in this region the selection of cluster members is limited to stars that are on the main sequence and have $P_{\mu} > 2\%$. From the combined CMD we deleted all stars below the main sequence and with $g' > 19$, except for a few very blue stars with $P_{\mu} \gtrsim 50\%$. Likewise, all stars with $g' > 16$ and located well above the main sequence and to the right of the RGB were eliminated. This leaves us with a total of 5699 probable cluster members.

3.1. Horizontal branch

The most prominent part of the horizontal branch (HB)—the red clump—contains 26 now kinematically-confirmed stars, consistent with the photometric selection by Kaluzny & Udalski (1992). More exciting is the presence of extreme horizontal branch (EHB) stars in NGC 6791, first recognized by Kaluzny & Udalski (1992). The following EHB stars are kinematic cluster members: B1,...,B7, B9 (names from Kaluzny & Udalski 1992; Kaluzny & Rucinski 1995). A much fainter star, B8, has a marginal $P_\mu=10\%$; however, its astrometry has large uncertainties and therefore we consider it to be a possible cluster member. In addition, star B16 ($P_\mu=59\%$) appears to be a cluster member and the following SBG stars are likely cluster members as well: S3472 ($P_\mu=98\%$), S13881 ($P_\mu=60\%$). The brightest UV-source, B10, (Landsman et al. 1998) is a definite field star. In Table 1 we provide two new EHB stars in NGC 6791, located at $R \sim 10'$.

Besides new EHB candidates, Table 1 lists a number of probable cluster members that we argue are classical HB stars. The bluest of these is the well-studied star 2-17 (Peterson & Green 1998), which is frequently assigned to the EHB. An intriguing feature of the HB here is an upturn at its red end. This could be the effect of duplicity among the red clump stars, although that may not be the only interpretation. We stress that proving the reality of the HB in NGC 6791 depends critically upon the ability to distinguish HB stars from blue stragglers.

There is one very bright star, S12158 ($V = 11.96$ $B - V = 1.24$), which is formally a probable cluster member ($P_\mu = 91\%$) but defies classification. Based on its possibly abnormally high luminosity, we consider it provisionally to be a field star.

3.2. Sub-subgiants

M67 is the first open cluster where the so-called sub-subgiants were discovered (Mathieu et al. 2003). These apparent binary stars occupy an area of the CMD below the subgiant branch, which is not easy to populate with any combination of two normal cluster stars. Owing to the low frequency of field stars in this part of the CMD, we are confident that at least five likely sub-subgiants are present in NGC 6791. In the notation of SBG, these are: S83, S746, S3626, S13753, and S15561. Three of these are also the known variable stars V17, V59, and 01431_10 listed by De Marchi et al. (2007). Only star V17 is in common with the alternative list of sub-subgiants (red stragglers) given by Kaluzny (2003).

4. Luminosity function and density profile

The depth and spatial extent of our survey allow the derivation of a reliable luminosity function (LF) for the entire cluster down to $g' \sim 24$. The only omissions are secondaries in binary stars and severe blends. We have counted all stars from the cropped CMD (Figure 1) in 0.5 mag bins, in two ways: star-by-star and by weighting each star with its membership probability (Figure 2). To translate g' into $M_{g'}$, an apparent distance modulus of 13.56 was applied. The peak at $M_{g'} \sim +4.5$ and the smooth downward trend toward fainter magnitudes is unmistakable. It is consistent with the appearance of the LF in King et al. (2005), although we cannot replicate the flattening of their LF at $g' > 22$ —even less so, the flat luminosity functions provided in Kaluzny & Udalski (1992) and Kaluzny & Rucinski (1995). A total of ~ 1000 cluster members per 1 mag bin around the main-sequence turnoff ($M_{g'} \sim +4.5$) in our present sample is a record high among the known old Galactic open clusters.

We constructed a (number) surface-density profile for NGC 6791 using the 4830 stars in Figure 1 brighter than $g' = 22$ (where the proper-motion discrimination between cluster members and field stars is best). This is shown in Figure 3. The filled circles in this plot show the number of stars per unit area, as a function of projected cluster-centric radius, defined by adding up stars weighted by their membership probabilities in a series of concentric circular annuli. The open circles result from adding up the total numbers of the same stars directly, without weighting by P_μ .

We fitted a single-mass, isotropic King (1966) model to the P_μ -weighted density profile in Figure 3, using only the data inside $R < 15'$ to constrain the fit. This implies a rather low central concentration for the cluster: $c \equiv \log(r_t/r_0) = 0.74 \pm 0.05$, corresponding to a dimensionless central King potential, $W_0 = 3.4 \pm 0.3$. The best-fitting King scale radius is $r_0 = 4'.22 \pm 0'.30$, which, given the low fitted concentration, implies a projected core (half-power) radius of $R_c = 3'.28 \pm 0'.12$. The associated tidal radius is $r_t = 23'.1 \pm 1'.0$, and the effective (projected “half-mass”) radius is $R_h = 4'.42 \pm 0'.02$ (it is normally the case that estimates of R_h are more robust than those of other characteristic radii). For a distance of 4.0 kpc to NGC 6791 (Grundahl et al. 2008), $1' = 1.16$ pc; thus, we have that the projected core radius of the cluster is $R_c \simeq 3.8$ pc; the effective radius is $R_h \simeq 5.1$ pc; and the fitted tidal radius is $r_t \simeq 27$ pc.

Fitting to various other number density profiles defined by both brighter and fainter magnitude cuts, and both weighted and not weighted by P_μ , yields results for R_c , R_h , and r_t that are generally compatible with the range of values suggested by the numbers just given for the $g' < 22$ case. The same is true for fits to luminosity surface-density profiles defined by adding up the luminosities of all the stars in our series of annuli. In exploring these various

definitions of the density profile, we saw a clear tendency for the inferred tidal radius (and thus the concentration, $\log(r_t/r_0)$) to increase systematically—along with R_h , to a lesser extent—as stars with fainter and fainter magnitudes were included to define the observed density profile. This is primarily because stars with $g' \gtrsim 19$ – 20 in our sample are somewhat depleted, relative to the brighter stars, in the innermost $\sim 2'$ – $3'$ of NGC 6791. However, it is not clear whether this is a physical effect (e.g., due to mass segregation) or an artifact of crowding and image blending in the core of the cluster.

The total luminosity of all stars with $g' < 22$ in our catalogue is $L_{\text{tot}} \approx 5500$ – $6500 L_{\odot, g'}$ (assuming $D = 4.0$ kpc, corrected for $A_{g'} = 0.55$ mag of extinction, and depending on whether or not the luminosities are weighted by P_{μ}). Adopting a theoretical g' stellar mass-luminosity relation from the Padova isochrones (Marigo et al. 2008) implies a total mass of $M_{\text{tot}} \approx 5000 M_{\odot}$ for the observed stars. This is a lower limit to the cluster mass because we have not attempted corrections for stellar binarity or incompleteness. We note that, if a King (1966) model with $c = 0.74$ and $R_h = 5$ pc accurately describes the internal mass profile of NGC 6791, then the projected, one-dimensional velocity dispersion averaged within the effective radius should be $\langle \sigma \rangle_h \simeq 0.36 (GM_{\text{tot}}/R_h)^{1/2} \approx 0.75 \text{ km s}^{-1}$. This corresponds to an intrinsic proper-motion dispersion of $\sigma_{\mu} \approx 0.04 (D/4 \text{ kpc})^{-1} \text{ mas yr}^{-1}$, which is much smaller than the formal uncertainties in our proper motions. It is also significantly lower than the radial-velocity dispersion of $\approx 2 \text{ km s}^{-1}$ reported for about a dozen red giants by Carraro et al. (2006), suggesting either that the Carraro et al. dispersion may be spuriously high, or that NGC 6791 may not be in virial equilibrium. Perhaps related to the second option, we note that a $5000 M_{\odot}$ cluster in a Galactic orbit with a pericenter of $\simeq 3$ kpc and an apocenter of $\simeq 10$ kpc (Bedin et al. 2006) is expected to have a tidal radius of $r_t \approx 13 \text{ pc} \simeq 11'$ at pericenter, and $r_t \approx 28 \text{ pc} \simeq 24'$ at apocenter—as against a value of $r_t \gtrsim 23'$ suggested by our King-model fitting of NGC 6791. Deciding the true dynamical state of this cluster will require much more comprehensive and higher-precision proper-motion and radial-velocity surveys, to obtain the tightest possible constraints on its orbit and to delineate accurately its internal kinematics.

5. Morphology of the red giant branch

Even a casual inspection of the cluster’s CMD reveals an unusually broad RGB – on the order of $\Delta(g' - r') \sim 0.1$ mag, while the formal uncertainties in the colors of these stars do not exceed ~ 0.02 mag. There is a variety of potential sources of increased scatter in the CMD, such as instrumental effects including the limitations of aperture photometry in crowded fields, presence of field stars, differential reddening, binarity of stars, metallicity variations,

and possible effects on color/luminosity of RGB stars by variable mass loss suggested by Kalirai et al. (2007).

Our proper-motion-vetted CMD offers a better look at the morphology of the RGB, which is more sensitive to differential reddening than the main sequence (apart from its turnoff region). In addition, our sample covers the largest area ever considered, thus enhancing the chances of finding the signs of differential reddening.

Unfortunately, we cannot take advantage of significantly reduced reddening effects in the near infrared. There is a poorly understood scatter in the $J - K$ color of our RGB stars from either 2MASS or Carney et al. (2005), which prevents us from using this color as a nearly reddening-free reference. Instead, we examined the morphology of the RGB branch in $g'r'$ CMD using approximately equal numbers of inner and outer probable cluster members by dividing the cluster at $R = 5'$. Then, we draw a ridge line for the inner sample, encompassing subgiants and RGB stars; see Figure 4. The majority of RGB stars at $R < 5'$ are bluer than this ridge line but, surprisingly, nearly all RGB stars at $R > 5'$ are redder than the ridge line of the inner sample. The shift in RGB color between the inner and outer samples is ~ 0.05 mag, whereas the age difference of 1 Gyr suggested by Twarog et al. (2011) would produce only a ~ 0.01 mag color shift in $g' - r'$ across the RGB region (Girardi et al. 2004). We conjecture that this color shift, at least in part, is due to differential reddening. Among the effects listed above, it is the only physical effect known to have an undeniable spatial dependency.

Our data provide evidence that differential reddening may not be ignored across the face of NGC 6791. Further advancements in our understanding of such a small effect require accurate near-infrared photometry and reliable identification of binaries in the upper part of the CMD.

6. Conclusions

This study provides a comprehensive and clean list of cluster members in one of the astrophysically most important Galactic star clusters. We hope that our findings in NGC 6791 and excellent cluster membership will stimulate in-depth future studies of individual cluster members.

We thank D. Crawford, J. Cummings, E. Hubbard, T. Kinman, B. Lynds, S. Majewski, R. Michie (deceased), K. Mighell, A. Sarajedini, and M. Sosey, whose time and effort at the telescope made this project possible. We thank the referee Barbara Anthony-Twarog

for pointing out the limitations of our data. This work has been supported in part by NSF grant AST 09-08114 to JHU (I.P.) and by NASA grant NNX09AH18A (The Kepler Open Cluster Study). Astrophysics at Keele University is supported by an STFC Rolling Grant. This study is based on observations obtained with MegaPrime/MegaCam, a joint project of Canada-France-Hawaii Telescope (CFHT) and CEA/DAPNIA, at the CFHT which is operated by the NRC of Canada, the Institut National des Sciences de l’Univers of the CNRS, and the University of Hawaii.

REFERENCES

- Bedin, L.R., Piotto, G., Carraro, G., King, I. R., & Anderson, J., 2006, *A&A*, 460, L27
- Boesgaard, A. M., Jensen, E. E. C., & Deliyannis, C. P. 2009, *AJ*, 137, 4949
- Borucki, W. J., et al., 2010, *Science*, 327, 977
- Carney, B. W., Lee, J.-W., & Dodson, B., 2005, *AJ*, 129, 656
- Carraro, G., Villanova, S., Demarque, P., McSwain, M. V., & Bedin, L. R., 2006, *ApJ*, 643, 1151
- Clem, J. L., VandenBerg, D. A., Stetson, P. B., 2008, *AJ*, 135, 682
- Cudworth, K. M., & Anthony-Twarog, B. J., 1993, *BAAS*, 25, 1454
- De Marchi, F., et al., 2007, *A&A*, 471, 515
- Girardi, L., Grebel, E. K., Odenkirchen, M., & Chiosi, C., 2004, *A&A*, 422, 205
- Grundahl, F., Clausen, J. V., Hardis, S. & Frandsen S. 2008, *A&A*, 492, 171
- Jones, B. F., & Walker M. F., 1988, *AJ*, 95, 1755
- Kalirai, J. S., Bergeron, P., Hansen, B. M. S., Kelson, D. D., Reitzel, D. B., Rich, R. M., & Richer, H. B., 2007, *ApJ*, 671, 748
- Kaluzny, J., 2003, *Acta Astron.*, 53, 51
- Kaluzny, J., & Rucinski, S. M., 1995, *A&AS*, 114, 1
- Kaluzny, J., & Udalski, A., 1992, *Acta Astron.*, 42, 29
- King, I. R., 1966, *AJ*, 71, 64

- King, I. R., Bedin, L. R., Pittto, G., Cassisi, S., & Anderson, J., 2005, *AJ*, 130, 626
- Kinman, T. D., 1965, *ApJ*, 142, 655
- Landsman, W., Bohlin, R. C., Neff, S. G., O’Connell, R. W., Roberts, M. S., Smith, A. M., & Stecher, T. P., 1998, *AJ*, 116, 789
- Magnier, E. A., & Cuillandre, J.-C., 2004, *PASP*, 116, 449
- Marigo, P., Girardi, L., Bressan, A., Groenewegen, M. A. T., Silva, L., & Granato, G. L. 2008, *A&A*, 482, 883
- Mathieu, R. D., 2000, in *ASP Conf. Ser. 198, Star Clusters and Associations: Convection, Rotation, and Dynamos*, R. Pallavicini, G. Micela, & S. Sciortino, San Francisco: ASP, 517
- Mathieu, R. D., van den Berg, M., Torres, G., Latham, D., Verbunt, F., & Stassun, K., 2003, *AJ*, 125, 246
- Meibom, S., & Kepler Team, 2010, *BAAS*, 42, 284
- Peterson, R. C., & Green, E. M., 1998, *ApJ*, 502, L39
- Scott, J. E., Friel, E. D., & Janes, K. A., 1995, *AJ*, 109, 1706
- Stetson, P. B., Bruntt, H., Grundahl, F., 2003, *PASP*, 115, 413
- Twarog, B. A., Carraro, G., & Anthony-Twarog, B. J., 2011, *ApJ*, 727, L7
- Zacharias, N., et al., 2010, *AJ*, 139, 2184

Table 1. New EHB candidates and our selection of HB stars

ID	RA (2000)	Dec (2000)	g'	$g' - r'$	P_μ (%)	Comment ^a
41698	290°2076111	37°6103973	20.291	−0.140	46	EHB candidate
58783	290.4511108	37.7326775	17.667	0.032	56	EHB candidate
45106	290.1308289	37.6360130	14.999	0.508	27	S2101
52460	290.0726929	37.6899757	15.116	0.845	42	S440
58857	290.2606201	37.7331924	15.186	0.530	99	3-22; RV=−2 var
60456	290.2799683	37.7429771	15.186	1.017	99	3-27
64067	290.1457214	37.7645378	15.253	0.387	99	S2746
64589	290.2497864	37.7675743	15.155	0.278	99	2-17; RV=−48
65895	290.2140503	37.7751503	14.785	1.075	99	NW-20; RV=−54
69734	290.2836304	37.7970619	14.568	1.096	99	3-33; RV=−20
69976	290.1916809	37.7985649	14.984	1.045	95	2-45; RV=−53
82982	290.3112488	37.8854256	15.276	0.901	53	S14140
89107	290.1376343	37.9322052	14.215	1.101	41	S2382
93625	290.4263306	37.9681969	15.165	0.590	58	

^aThe SBG numbers are preceded by a letter S; remaining cross-identifications are from Kinman (1965); radial velocity (RV) in km s^{-1} is from the literature.

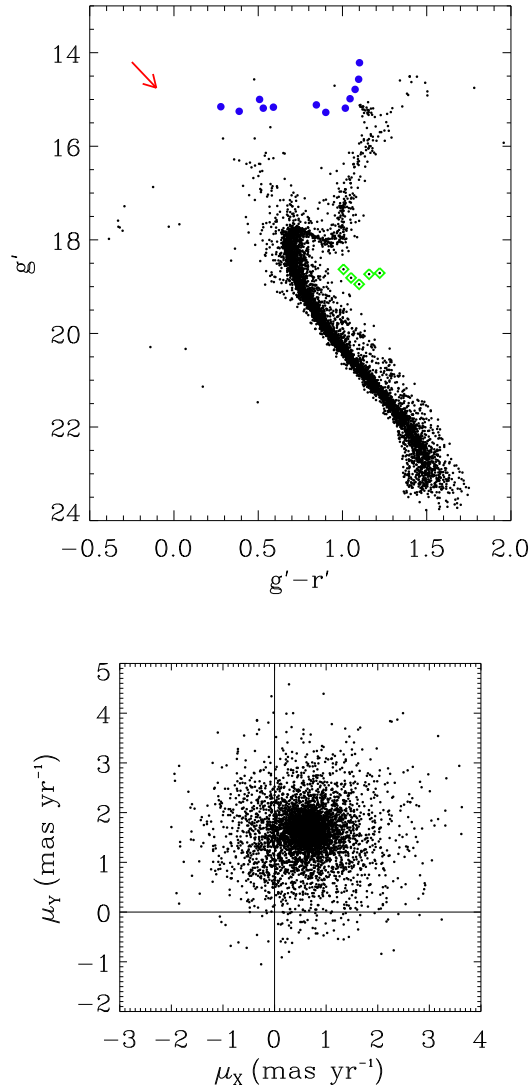


Fig. 1.— Color-magnitude and vector-point diagrams of NGC 6791. Upper panel: CMD of all probable cluster members, with the exception of some cropped areas. The large dots indicate our selection of HB stars; the rombs show the proposed sub-subgiants. The arrow shows the direction and the adopted total amount of reddening [$E(g' - r') = 0.145$, $A_{g'} = 0.55$, following Grundahl et al. (2008)]. Lower panel: relative proper motions of probable cluster members only. The larger spread of the outer points reflects the relatively low precision of proper motions near the limit of the catalog at $g' = 23.5$.

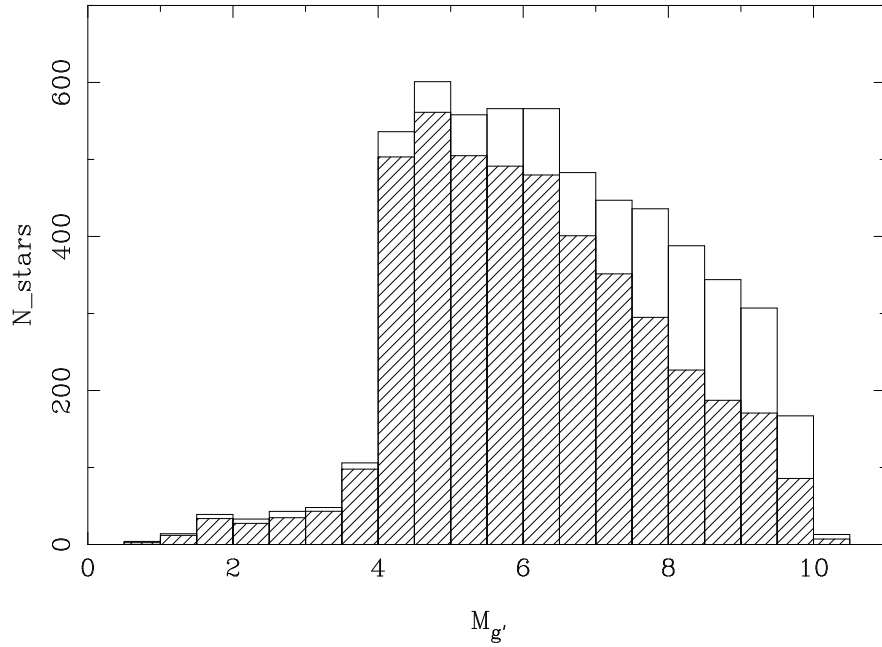


Fig. 2.— Luminosity function of NGC 6791. Each bin is 0.5 mag wide. The hatched histogram is obtained by weighting each star, shown in Figure 1, with its membership probability (P_{μ}), while the open histogram shows the the actual numbers of stars without weighting by P_{μ} . The last two bins at absolute magnitude $M_{g'} \sim +10$ are incomplete.

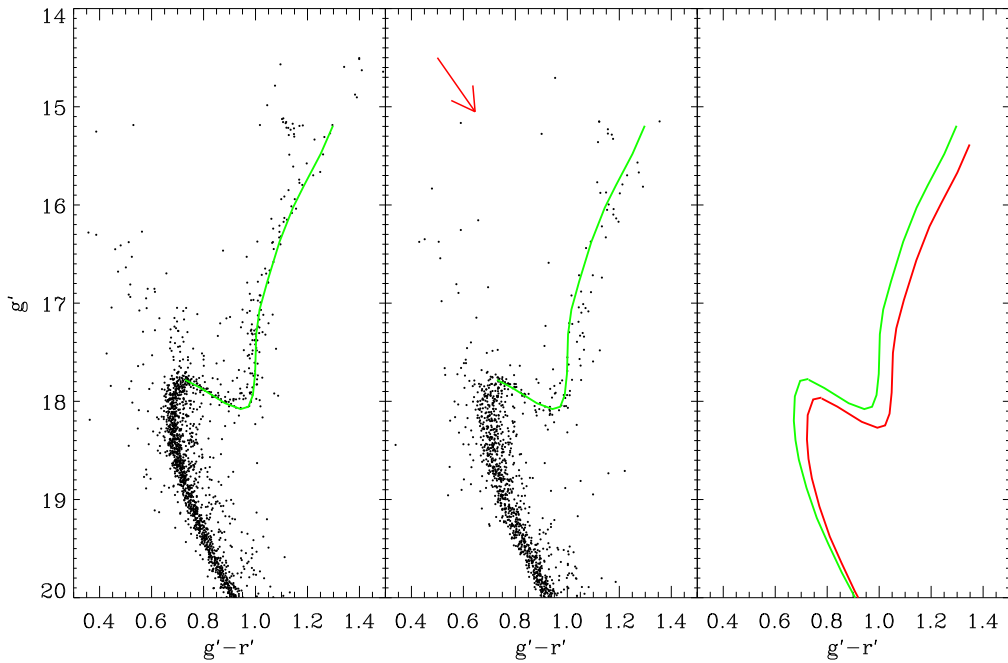


Fig. 4.— Color-magnitude diagram of NGC 6791 with emphasis on RGB. The left panel shows a CMD for the inner cluster sample ($R < 5'$); the middle panel, for the outer sample ($R \geq 5'$). For the arrow, see Figure 1. In both panels, the curve indicates the location of inner sample’s ridge line for subgiants and RGB stars. Note the location of RGB stars relative to this ridge line. The right panel elucidates the effect of a reddening $E(g' - r') = 0.05$ applied to the cluster’s inner-sample fiducial. This loosely characterizes the degree of differential reddening in NGC 6791.